Buletinul Ştiinţific al Universităţii "Politehnica" din Timişoara

Seria ELECTRONICĂ şi TELECOMUNICAŢII
TRANSACTIONS on ELECTRONICS and COMMUNICATIONS

Tom 58(72), Fascicola 1, 2013

Estimation of Automotive Target Trajectories by Kalman Filtering

Adrian Macaveiu[1] Andrei Campeanu[1] Ioan Nafornita[1]

Abstract – 24- and 77-GHz automotive radar sensors have been introduced into series production by car manufacturers. An application aiming to increase traffic safety consists in detecting and tracking Vulnerable Road Users (VRU) and vehicles in front of the car. This is achieved by using a single 24-GHz radar sensor, capable of measuring range, radial velocity and azimuth angle even in multiple target scenarios. In this paper a signal processing algorithm for target tracking is presented. Target position and speed in Cartesian coordinates are estimated with the aid of a Kalman filter. The work is developed under the FP7 EC funded project ARTRAC.
Keywords: Tracking, Kalman filter, automotive radar

I. INTRODUCTION

Advanced Driver Assistance Systems are based on automotive radars in the 24- and 77-GHz band because of their capability to operate in all weather and lighting scenarios and because they are cheaper than infrared or video based systems.
This paper focuses on the use of 24-GHz radars for target tracking with the aid of Kalman filters. Different types of waveforms which can be used in 24-GHz automotive radars are reviewed in section II. Section III gives a possible signal processing structure for tracking based on raw detections provided by the sensor. An important part of the algorithm is the Kalman filter used to estimate the current target parameters and to predict the new set of parameters for the next iteration. The filter needs to be flexible enough to deal with several types of target trajectories with variable speed, so care must be taken in choosing the appropriate parameters in the filter design stage. We have generated a number of different target movement paths in order to test the Kalman filter concerning its capabilities to estimate target position and velocity. Section IV presents the scenarios considered for testing and the tracking results, while section V summarizes the conclusions.

II. AUTOMOTIVE RADAR WAVEFORMS

In order to measure target range and velocity a suitable waveform needs to be designed. The classical pulse waveform (Fig. 1) uses the time delay between the transmitted and received pulses to calculate the target range, and the Doppler frequency to measure the velocity, but it generates high computational complexity, so it is not suitable for automotive radar applications [1].

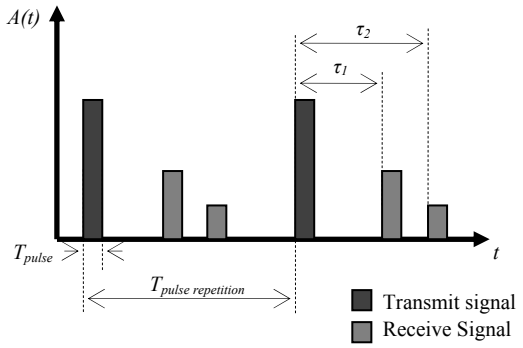

Fig. 1. Pulse radar waveform

To achieve low measurement time and to overcome the drawback of pulse waveforms, the continuous wave (CW) radar was introduced. There are two main types of CW waveforms: the linear frequency modulated (LFM) and the frequency shift keying (FSK), both presented in Fig. 2.
When using the LFM waveform, there is a frequency shift produced by two causes: the time delay of the received echo signal and the Doppler-Effect. Thus, the range and velocity cannot be determined unambiguously from a single chirp signal. Multiple target scenarios produce ghost targets in the range-velocity plane. This is partly resolved by considering the FSK waveform, where we can measure the Doppler frequency from the two different frequency signals by applying an FFT.

[1] Faculty of Electronics and Telecommunications, Communications Dept.
Bd. V. Parvan 2, 300223 Timisoara, Romania, e-mail {adrian.macaveiu,andrei.campeanu,ioan.nafornita}@upt.ro

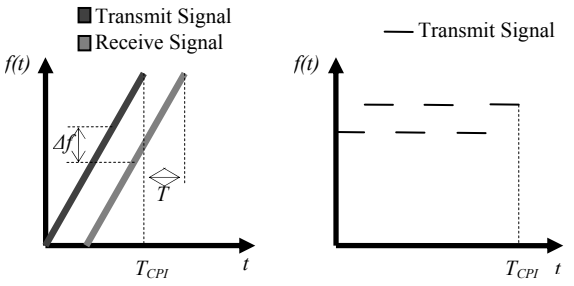

Fig. 2. LFM and FSK waveforms

The phase shift between the echoes of the two alternating signals introduced by the time delay of the received signal allows range measurement. The drawback of the FSK waveform is that it cannot resolve stationary targets. Also, it offers no range resolution, meaning it is not able to detect multiple targets.

For multiple target situations, a variant of the LFM technique described in [2] and [3] is applied, by transmitting a number of chirps with different frequency modulations, translating in different sweep rates (Fig. 3). The drawback of this type of waveform is the extended measurement time.

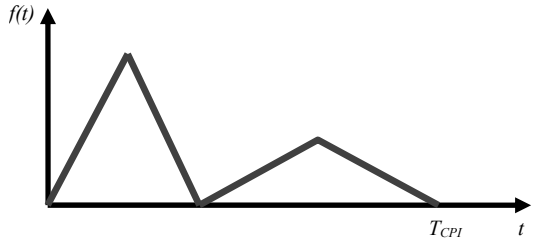

Fig. 3. LFM waveform used in multiple target situations

The combination between FSK and LFM waveform principles, presented in [2] and [4] enables unambiguous range and velocity measurements in multiple target scenarios with the advantage of a shorter measurement time. The concept is shown in Fig. 4 and it is called MFSK. It consists of two stepwise linearly modulated signals with a frequency shift between them. They are transmitted in an intertwined way. The frequency difference (beat frequency) obtained from the received signal contains information about range and velocity. The phase shift between the two signals *A* and *B* measured at the beat frequency also depends on range and velocity. Thus, a linear system of two equations can be solved for finding the two parameters of interest unambiguously even in multiple target environments.

Current research projects, like the one described in [5], use a sequence of consecutive chirps as a transmit signal (Fig. 5). In order to avoid making the difficult phase difference measurement, this method makes use of two FFT operations. The first one is done on each received chirp to find the beat frequency and it gives information about targets placed at different ranges. The second FFT is performed for each range gate (which has samples from every chirp) to determine the Doppler frequency and thus detect targets with

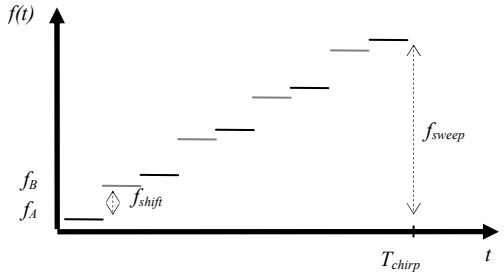

Fig. 4. MFSK waveform

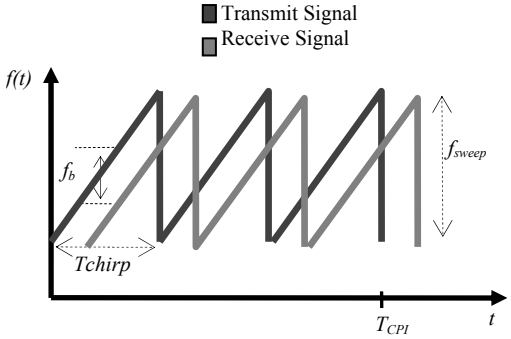

Fig. 5. The rapid chirp waveform

different radial velocities in the same range gate. The resulting range-velocity diagram has no ambiguities.

III. SIGNAL PROCESSING STRUCTURE

We have proposed the signal processing algorithm given in Fig. 6 for estimating target range and velocity and performing the tracking operation for detected objects.

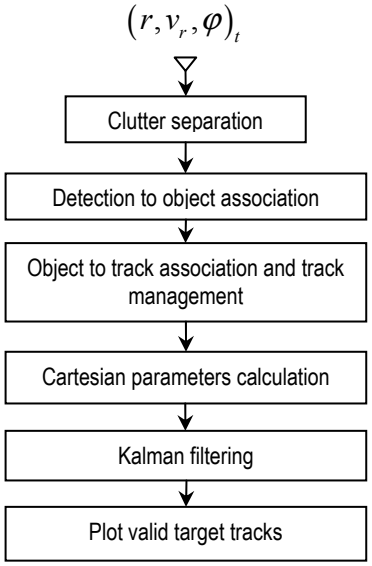

Fig. 6.Signal processing scheme

The radar measures the target range *r,* the radial velocity v_r and the azimuth angle φ at measurement

timestamp *t*. Besides the detections which correspond to real targets, there are also reflections coming from the surrounding environment such as trees, buildings or traffic signs. These detections need to be filtered out so they are not fed to the following processing blocks. All of the unwanted detections are labeled as clutter, and they are eliminated by evaluating their radial velocity. At this point, scenarios with a stationary ego vehicle are considered, so it is appropriate to declare that a very slow moving or stationary detection is actually clutter and needs to be left out. In more complicated scenarios where the ego vehicle is also maneuvering with a certain speed and yaw rate, compensation is needed in both radial velocity and azimuth angle for all detections in order to obtains their position parameters relative to the road coordinate system and the actual velocity.

Research in this field has reported that the targets detected by an automotive radar sensor exhibit modified range and Doppler profiles than usual radar targets. Indeed, experiments have shown that in general, a longitudinally moving vehicle has an extended range profile due to its size in comparison to the radar range resolution (which can be smaller than 1 m). On the other hand, a vehicle has a point-shaped velocity profile since the radar sees a single "block" travelling at one speed. In opposition to this, a laterally moving pedestrian (the usual street crossing scenario) has a point shaped range profile and an extended velocity profile because it has three parts which "move" with different frequencies: the arms, torso and legs [6]. This difference between target types enables the feature extraction which can be used to classify detected targets, thus making the automotive radar a suitable tool for pedestrian recognition. Another remark is that in these types of scenarios the target usually has multiple reflection points.

Based on the above observations, a first detection-to-object data association block has been integrated to make sure that multiple detections from the same target are grouped into the same object. This is done by building a gate around the object in the three-parameter space and analyzing which detections fall into that gate. The result of this procedure is a list of objects which can then be associated with the existing tracks by using a nearest neighbor technique. A new track is initialized if the current object does not belong to any existing track. Inevitably the outcome of this block will contain a number of false tracks in addition to the true target track. Only the tracks corresponding to real targets will be fed to the Kalman filtering algorithm.

The challenge in automotive radar systems is the ability to successfully determine the tracks for all detected targets in real traffic, multiple target scenarios. In this case, the data association procedure becomes more complicated since it needs to deal with objects which are randomly appearing, disappearing or occluding each other in the radar field of view. A more suitable data association algorithm called the Hungarian algorithm is presented in [7] and can be applied to object tracking in Cartesian coordinates.

The Kalman filtering stage has two goals: the first is to offer an estimation of the target position and speed at the current timestamp *t*. The second goal is to make a prediction about these parameters for the next timestamp *t+1* which will be used to minimize the estimation error at the next iteration when new measurements will be available. The solution is computed in a recursive manner [8], [9].

Based on the theoretical groundwork set in [10] we have implemented in this paper a linear Kalman filter which processes target range and velocity in Cartesian coordinates. Therefore, the system state at the current timestamp is given by:

$$\mathbf{x} = \begin{bmatrix} x & v_x & y & v_y \end{bmatrix}', \tag{1}$$

where ' denotes the transpose.

The target movement is described by a constant velocity model. This means that the state prediction for timestamp *t* based on the previous state estimation at *t-1* is given by:

$$\mathbf{x}_t = \mathbf{A} \cdot \mathbf{x}_{t-1} + \mathbf{w}_{t-1}, \tag{2}$$

which is equivalent to:

$$\begin{bmatrix} x \\ v_x \\ y \\ v_y \end{bmatrix}_t = \begin{bmatrix} 1 & T & 0 & 0 \\ 0 & 1 & 0 & 0 \\ 0 & 0 & 1 & T \\ 0 & 0 & 0 & 1 \end{bmatrix} \cdot \begin{bmatrix} x \\ v_x \\ y \\ v_y \end{bmatrix}_{t-1} + \begin{bmatrix} 0 \\ w_x \\ 0 \\ w_y \end{bmatrix}_{t-1}, \tag{3}$$

where $\mathbf{w}_{t-1}$ is the Gaussian state noise vector of zero mean and $\mathbf{E}_x$ covariance matrix. **A** represents the state transition matrix and *T* is the measurement period, chosen to be equal to 38 ms, according to the analysis made in [11] for the MFSK waveform.

Because we need to estimate both target position and speed in Cartesian coordinates, the measurement matrix of the Kalman filter is built accordingly, to specify that both sets of parameters are being measured:

$$\mathbf{H} = \begin{bmatrix} 1 & 0 & 0 & 0 \\ 0 & 1 & 0 & 0 \\ 0 & 0 & 1 & 0 \\ 0 & 0 & 0 & 1 \end{bmatrix}. \tag{4}$$

The measurement equation at timestamp *t* is given by:

$$\mathbf{z}_t = \mathbf{H} \cdot \mathbf{x}_t + \mathbf{n}_t, \tag{5}$$

where **n** is the measurement noise vector, which has zero expectation and $\mathbf{E}_z$ covariance matrix.

The values for the measurement and state noise covariance matrices are chosen in the following way:

as in a practical scenario, the measurements are highly affected by noise, so we assign large values to $\mathbf{E}_z$. We also keep in mind that the speed measurements are more inaccurate that the range measurements. This means that the variance of the speed measurements should be larger than the variance for the range measurements. As a general rule, large values of the measurement noise covariance matrix mean that the state estimation is based more on the state prediction model than on the measured parameters. The output of this assumption is that the track will be smoother, so the noise is properly removed, but the filter will not be able to follow fast variations of position and speed with great accuracy. The simulated tracks are generated in such a way that they fit into the assumptions above. On the other hand, if the measurements are noisy, we need an accurate model for the target movement. This means that the state noise covariance matrix will have small values, so the filter is able to correct the deviations in the measurements based on the state transition model. In both cases we have assumed that the variables affected by noise are uncorrelated, so both covariance matrices have diagonal form.

The Kalman equations describe the prediction of the current state and the state estimation update:

$$\begin{aligned}
\overline{\mathbf{x}}_t &= \mathbf{A}\cdot\mathbf{x}_{t-1} \\
\overline{\mathbf{P}}_t &= \mathbf{A}\cdot\mathbf{P}_{t-1}\cdot\mathbf{A}^T + \mathbf{E}_x \\
\mathbf{K}_t &= \overline{\mathbf{P}}_t\cdot\mathbf{H}^T\cdot\left(\mathbf{H}\cdot\overline{\mathbf{P}}_t\cdot\mathbf{H}^T + \mathbf{E}_z\right)^{-1}, \quad (6) \\
\mathbf{x}_t &= \overline{\mathbf{x}}_t + \mathbf{K}_t\cdot\left(\mathbf{z}_t - \mathbf{H}\cdot\overline{\mathbf{x}}_t\right) \\
\mathbf{P}_t &= \left(\mathbf{I} - \mathbf{K}_t\cdot\mathbf{H}\right)\cdot\overline{\mathbf{P}}_t
\end{aligned}$$

where $\mathbf{K}$ denotes the Kalman gain, $\overline{\mathbf{P}}$ is the predicted covariance matrix of the error and $\mathbf{P}$ is the covariance matrix of the state estimation error.

IV. SIMULATION RESULTS

The MATLAB environment was used to test the proposed tracking solution. Different situations were generated by simulating various target movement trajectories. The algorithm estimates the target position and speed in Cartesian coordinates. The measurement cycle was chosen to be 38 ms, according to existing 24 GHz automotive radar specifications. We have generated 500 samples of received data, yielding a total of 19 s of recorded radar measurements. The ego vehicle is assumed to be stationary and a single valid target is considered. Depending on the speed, we can consider that the target can be associated with either a vehicle or a pedestrian in real traffic scenarios.

The first scenario simulates a longitudinally moving target that is moving away from the ego vehicle with a speed of v_y = 10 km/h and v_x = 0. The tracking results are presented in Fig. 7. The 'x' markers represent the single measurements provided by the radar, the real target behavior is shown in black, while the Kalman filter output is represented in red.

It can be seen in Fig. 7a that the noise is removed successfully up to a point where the maximum error between the estimation and the real target position is much smaller than 1 m, which is the radar range resolution according to the specification in [5]. The speed estimation also gives good results, as can be seen in Fig. 7b and Fig. 7c. The lateral speed is zero because the vehicle is moving in a straight line away from the ego vehicle at zero azimuth angle.

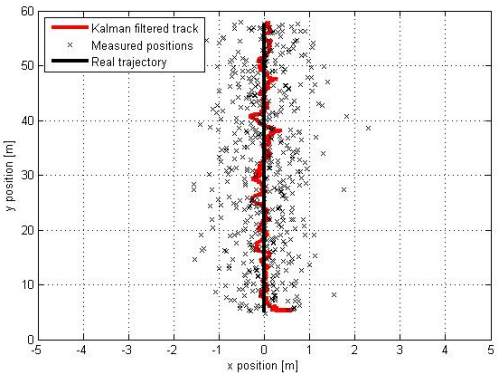

Fig. 7a. Position estimation

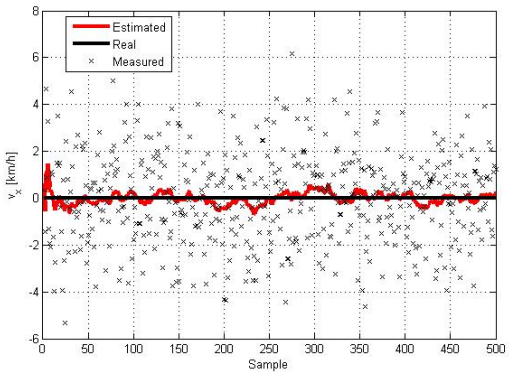

Fig. 7b. Speed estimation - v_x

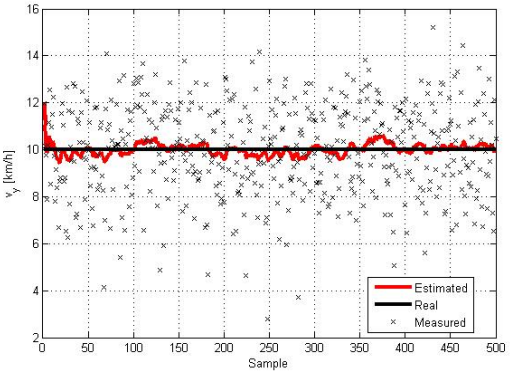

Fig. 7c. Speed estimation – v_y

Next, a laterally moving target scenario was tested. The target is passing in front of the ego vehicle in a straight line at v_x = 5 km/h. This time v_y = 0. The results are presented in Fig. 8.

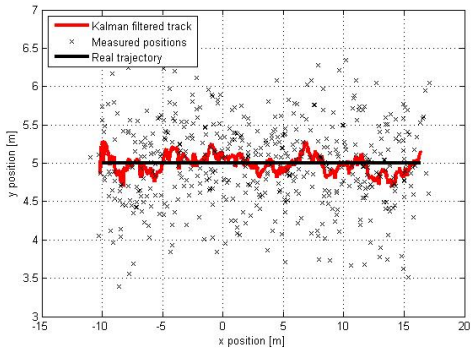

Fig. 8a. Position estimation

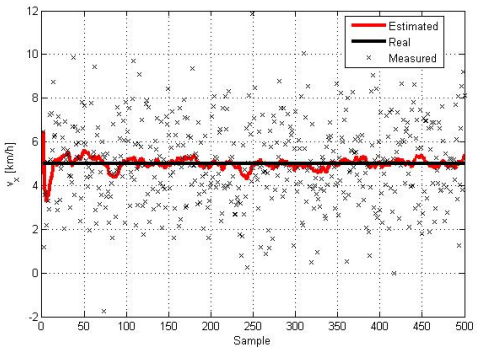

Fig. 8b. Speed estimation - v_x

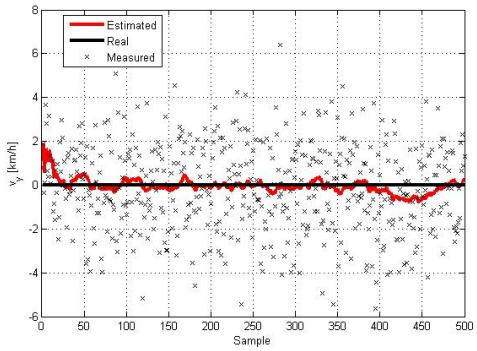

Fig. 8c. Speed estimation – v_y

The next scenario depicts a target moving diagonally with respect to the ego vehicle, at v_x = -2 km/h and v_y = 10 km/h. The results are shown in Fig. 9.

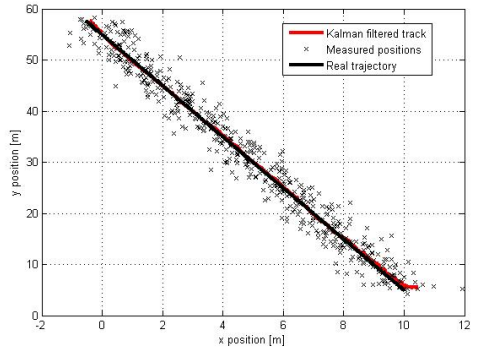

Fig. 9a. Position estimation

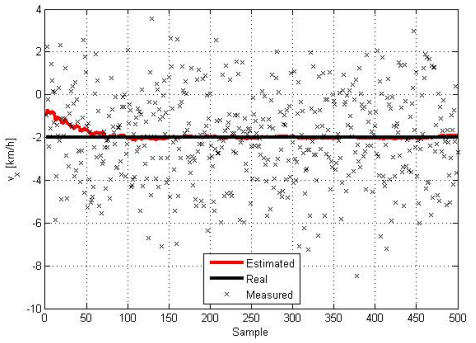

Fig. 9b. Speed estimation - v_x

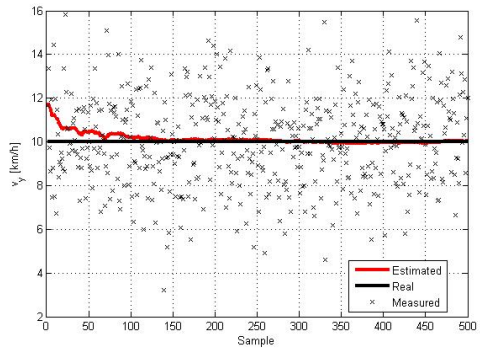

Fig. 9c. Speed estimation – v_y

The next case shows a target performing a turn while passing in front of the ego vehicle: v_x varies linearly from -5 to 5 km/h while v_y = 10 km/h (Fig. 10).

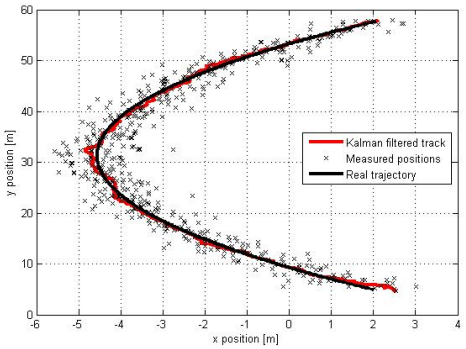

Fig. 10a. Position estimation

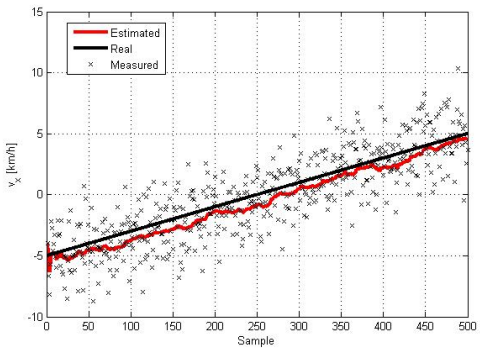

Fig. 10b. Speed estimation - v_x

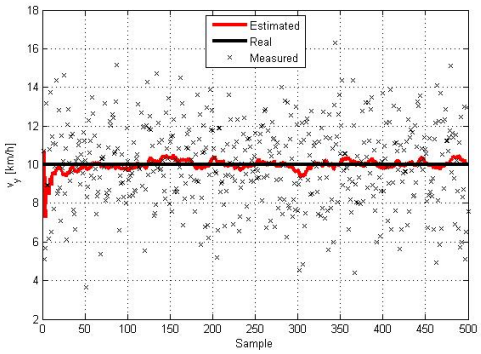

Fig. 10c. Speed estimation – v_y

The final scenario depicts a target which performs a direction change and then resumes back to its lane: v_y has a sinusoidal variation of amplitude 1.5 km/h and v_x = 5 km/h. The results are presented in Fig. 11.

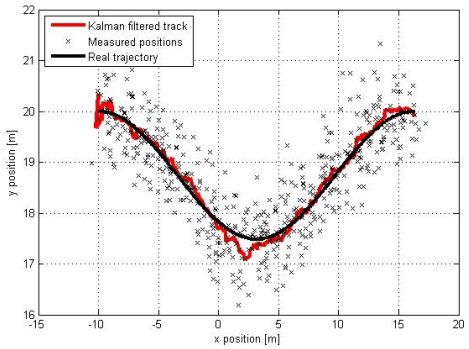

Fig. 11a. Position estimation

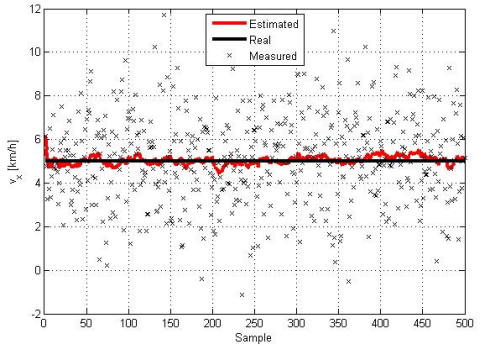

Fig. 11b. Speed estimation - v_x

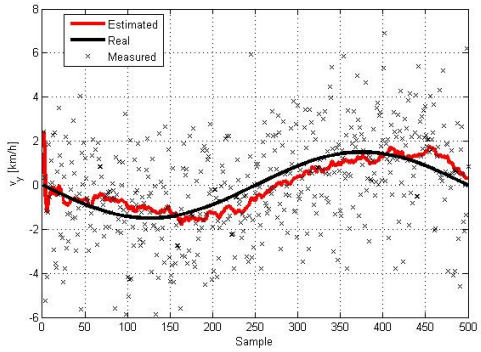

Fig. 11c. Speed estimation – v_y

It can be seen that the speed estimation error becomes larger when the variation law is more complicated (Fig. 10b and Fig. 11c). This means that the tracker is not entirely able to follow the fast speed variations with the Kalman parameters chosen in this simulation. However, the position estimation is very good in all cases, with the maximum error being smaller than the radar range resolution.

V. CONCLUSIONS

Driver Assistance Systems use 24- and 77-GHz radar sensors. There has been a significant evolution in the waveforms used for such sensors, from the classical pulse to the modern rapid chirp waveform, which enables unambiguous range and velocity measurements in multiple target scenarios and has a short measurement cycle.

A tracking algorithm using a linear Kalman filter was implemented in this paper and tested with simulated target trajectories, aiming to estimate position and speed. The results of position estimation are good considering the simplicity of the target motion model, with the maximum error complying with existing specifications concerning the radar range resolution. The speed estimation results also look promising. In more complicated scenarios where the target is maneuvering faster and the speed variation is rapid, the speed estimation error is larger, but results could be improved by careful selection of the Kalman algorithm parameters.

REFERENCES

[1] H. Rohling, "Milestones in Radar and the Success Story of Automotive Radar Systems", *Proceedings of the International Radar Symposium,* Vilnius, Lithuania, 2010.

[2] H. Rohling, M.-M. Meinecke, "Waveform Design Principles for Automotive Radar Systems", *Proceedings of the CIE International Conference on Radar,* Beijing, China, 2001.

[3] K. Pourvoyeur, R. Feger, S. Schuster, A. Stelzer, L. Maurer, "Ramp Sequence Analysis to Resolve Multi Target Scenarios for a 77-GHz FMCW Radar Sensor", *11th International Conference on Information Fusion,* Cologne, Germany, 2008.

[4] M.-M. Meinecke, H. Rohling, "Combination of LFMCW and FSK Modulation Principles for Automotive Radar Systems", *German Radar Symposium GRS2000,* Berlin, Germany, 2000.

[5] H. Rohling et al., "The ARTRAC Architecture", http://artrac.org/file.php/ARTRAC_Architecture.pdf-2012-10-16 , last accessed on 05.12.2013.

[6] S. Heuel, H. Rohling, "Two-Stage pedestrian classification in automotive radar systems", *18th International Radar Symposium*, pp. 477-484, Leipzig, Germany, 2011.

[7] H. W. Kuhn, "The Hungarian method for the assignment problem", *Naval Research Logistics*, Vol. 52, pp. 7-21, Wiley Periodicals, 2005.

[8] P. Kim, *Kalman Filters for Beginners: with MATLAB Examples,* translated by Lynn Huh, CreateSpace, 2011.

[9] A. Campeanu, J. Gál, *Adaptive signal processing methods,* Timisoara, Ed. Politehnica, 2009 (in Romanian language).

[10] Y. Bar-Shalom, X. Rong Li, T. Kirubarajan, *Estimation with Applications to Tracking and Navigation: Theory Algorithms and Software,* New York, John Wiley & Sons, 2001.

[11] S. Heuel, H. Rohling, "Pedestrian Recognition in Automotive Radar Sensors", *14th International Radar Symposium,* Dresden, Germany, 2013.